Analysis of the SEIR Model for Measles Spread with the Influence of Vaccination

Joseph Leonardo Marvin Hamzah, Helisyah Nur Fadhilah*, and Rindra Syaifullah,

***Abstract*—In this paper, we analyze the impact of vaccination on the dynamics of measles transmission using the SEIR mathematical model. We demonstrate that high vaccination coverage significantly reduces disease transmission and establishes herd immunity, thereby protecting both vaccinated and unvaccinated populations. We observe that low to moderate vaccination levels result in an increase in the reproduction number, leading to periodic outbreaks, especially in communities with low vaccine uptake. Our analysis identifies both adult and child vaccination rates as critical factors in stabilizing disease dynamics. In the absence of vaccination, we observe uncontrolled outbreaks that pose significant risks to public health. These findings underscore the importance of implementing robust vaccination programs to prevent measles outbreaks and maintain public health stability.**

***Index Terms*—Measles, SEIR Model, Vaccination, Disease Transmission.**

I. Introduction

Measles is a highly contagious disease with the highest susceptibility rate of any disease worldwide. It is characterized by symptoms such as fever, sore throat, and a rash covering the entire body. Measles has a significant potential to cause outbreaks and is endemic in nature. Children who are not vaccinated are extremely vulnerable to contracting measles. Before the advent of immunization, nearly all children globally were affected by measles. Measles is considered dangerous because it can lead to complications such as brain damage, damage to other organs, lifelong disabilities, paralysis, and even death [1].

The advancement of scientific knowledge is crucial in preventing the spread of measles. Mathematical models have become a crucial tool for understanding the transmission dynamics of epidemic diseases and for suggesting control strategies to manage them [2]. Such models can aid in predicting and controlling measles in the future. The foundational model for disease spread was introduced by Kermack in 1927 [3]. This model is known as the SIR model, where S, I, and R stand for Susceptible (the healthy population that is vulnerable to the disease), Infected (the number of individuals currently infected), Recovered (the number of individuals who have recovered and are immune to the disease) respectively. In this paper we use SEIR model, which is a modification of the SIR model. These are individuals who have been exposed (E) to the virus but are not yet infectious [4].

Measles has a latent period, which is the time between infection and the appearance of symptoms. This latent period introduces a new class, E (Exposed), representing the number of individuals who have been exposed to the disease but have not yet shown symptoms. Consequently, the model evolves from SIR to SEIR to accommodate this new class.

Studying measles outbreaks can provide valuable data on disease transmission, patterns of infection, and vulnerable populations, aiding in the development of targeted prevention strategies [5]. Measles vaccination programs have been highly effective in reducing the global burden of the disease. Analyzing vaccination coverage and its impact on disease prevalence helps evaluate the success of immunization efforts [6]. Measles outbreaks often prompt public health responses such as vaccination campaigns, quarantine measures, and educational initiatives. Analyzing these responses can inform future policy decisions and improve outbreak control strategies [7]. Measles is a classic example of a disease where herd immunity plays a crucial role. Analyzing the threshold for herd immunity and factors influencing it can guide vaccination strategies to protect vulnerable populations [8]. Measles remains a significant cause of morbidity and mortality in many parts of the world. Analyzing its impact on global health helps prioritize resources for disease prevention and control efforts.

In this paper, we also study the basic reproduction number (R_0). The study of basic reproduction number estimates for a measles disease model can be found in the article by authors in [9]. The article reveals that from 18 reviewed literatures, it can be concluded that there are 58 estimates for the basic reproduction number of measles. Studying measles outbreaks provides valuable data on disease transmission, patterns of infection, and vulnerable populations, which aids in developing targeted prevention strategies [5]. Vaccination programs have proven highly effective in reducing the global burden of measles. Analyzing vaccination coverage and its impact on disease prevalence helps evaluate the success of immunization efforts [6]. In this paper, we use the reproduction number under vaccination (R_v) to reflect the potential for disease spread in a vaccinated population [9]. Understanding its dynamics is vital for assessing vaccination effectiveness. A lower R_v indicates that high vaccination coverage can significantly curb disease transmission, thus protecting both vaccinated and unvaccinated individuals.

Moreover, we analyze elasticity measures concerning

Manuscript received July 8, 2024; revised December 20, 2024.

Joseph Leonardo Marvin Hamzah is an undergraduate student of Department of Data Science, School of Computing, Telkom University, Surabaya, Indonesia (e-mail: josephleoanrdo@student.telkomuniversity.ac.id).

Helisyah Nur Fadhilah is a lecturer of Department of Data Science, School of Computing, Telkom University, Surabaya, Indonesia (corresponding author to provide e-mail: helisyahnf@telkomuniversity.ac.id).

Rindra Syaifullah is an undergraduate student of Department of Data Science, School of Computing, Telkom University, Surabaya, Indonesia (e-mail: rinsyaf@student.telkomuniversity.ac.id).

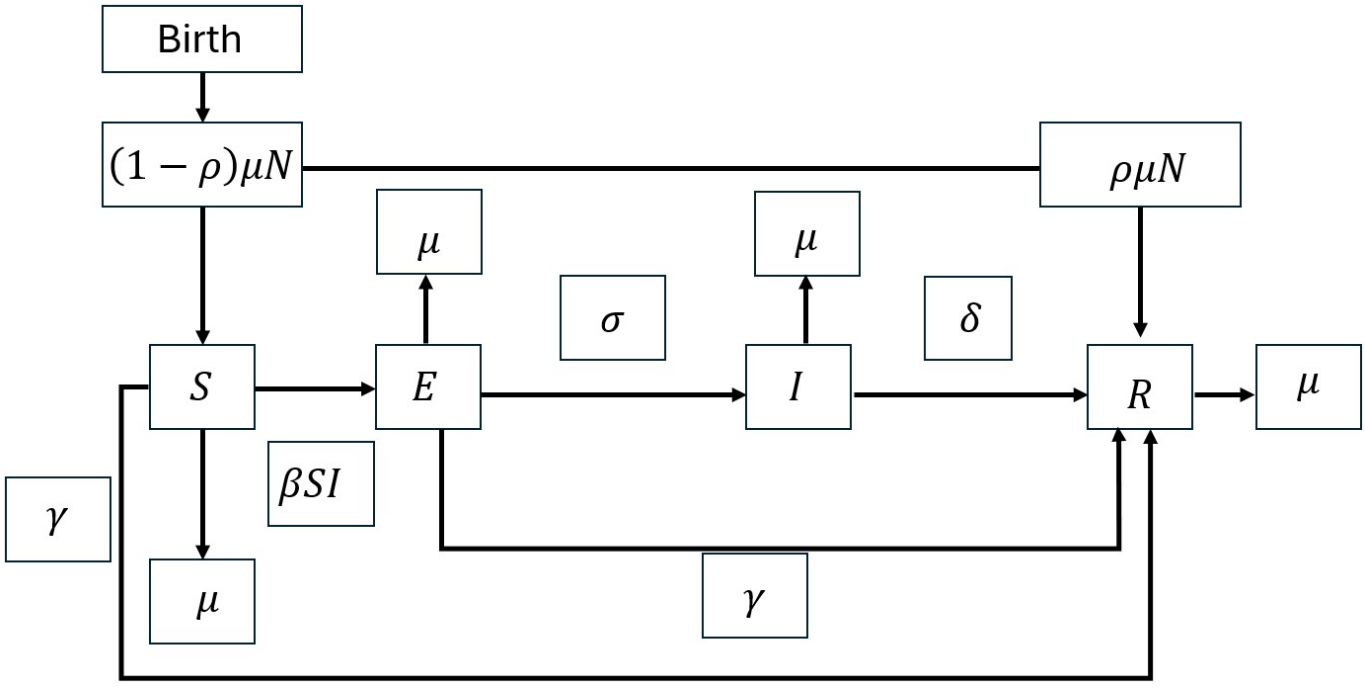

Fig. 1: Compartment of Measles Disease Spread Model.

changes in vaccination rates for adults and children, to demonstrate how sensitive disease dynamics are to shifts in these parameters. High elasticity values signify that fluctuations in vaccination rates can substantially influence the overall spread of measles, underscoring the importance of maintaining high vaccination coverage.

II. SEIR MATHEMATICAL MODEL

In this case, Figure 1 helps in understanding the dynamics of disease transmission by providing a framework to analyze how individuals transition between these compartments over time. In this case the individuals can move between these compartments over time based on different rates and probabilities. S (Susceptible), represents the portion of the population that is susceptible to the infection but has not yet been exposed. βSI is the rate at which susceptible individuals become exposed when they come into contact with infectious individuals. Here, β is the transmission rate, and SI represents the interaction between susceptible (S) and infected (I) individuals. Lastly μ is the natural death rate from the susceptible group due to causes other than measles.

Additionally, diseases like measles have a latent period that creates a new class, exposed (E). Exposed represents an individual who has been exposed to the infection but is not yet infectious or incubated. σ is the rate at which exposed individuals become infectious, or in other word move from E to I. This is the inverse of the incubation period. I represents an individual who is actively infected and capable of transmitting the disease to others. δ is the recovery rate, which represents the rate at which infectious individuals recover and move to the recovered (R) compartment.

R represents an individual who has recovered from the disease or has been removed either by death or other factors and is assumed to have immunity. $\rho\mu N$ is the rate of entry into the recovered compartment, which may involve births of immune individuals. Birth represents the inflow of new individuals into the susceptible population. $(1-\rho)\mu N$ is the portion of infant that enter the susceptible group, where ρ represents the fraction of individuals who are vaccinated. γ represents the rate of vaccination for adults, moving individuals from the susceptible population directly to the recovered population, thereby reducing the number of people vulnerable to infection. μN is the total birth rate. The total number of individuals is $s+e+i+r=1$ where, $s=\frac{S}{N}, e=\frac{E}{N}, i=\frac{I}{N}, r=\frac{R}{N}$ and we obtain the following equation

$$\frac{ds}{dt} = (1-\rho)\mu - (\beta i+\mu+\gamma)s, \quad (1)$$

$$\frac{de}{dt} = \beta si - (\mu+\gamma+\sigma)e, \quad (2)$$

$$\frac{di}{dt} = \sigma e - (\mu+\delta)i, \quad (3)$$

$$\frac{dr}{dt} = \rho\mu + e\gamma + \delta i - \mu r + \gamma s. \quad (4)$$

The mathematical model for the spread of measles 1-4 are constructed based on population compartments as explained in Figure 1.

A. Reproduction number with the next generation matrix method

The next generation matrix is widely used in epidemiology to compute the basic reproduction number R_0 for infectious

diseases. R_0 represents the average number of secondary infections caused by a single infectious individual in a completely susceptible population. This method helps estimate R_0 from a SEIR model in equation 1-4. The system has a disease-free equilibrium (DFE) at $(S, I, E, R) = (S_0, 0, 0, 0)$, where the DFE is locally asymptotically stable (LAS) if $R_0 < 1$, but unstable if $R_0 > 1$ [10].

The basic reproduction number R_0 is determined by the transmission rate, the average duration of infectiousness, and the initial susceptible population S_0. Notably, R_0 is unaffected by the proportion of individuals who die from the disease. When R_0 is less than 1, the number of infectious individuals steadily decreases until the disease is eliminated. However, when R_0 is greater than 1, the infection initially spreads before eventually declining to zero. Therefore, $R_0 = 1$ marks the critical point between the disease dying out and the potential for an epidemic [11].

The infection matrix F describes the new infections in each infected compartment. Elements F_{ij} of the matrix represent the rate at which individuals in compartment i produce new infections in compartment j. Transition matrix V describes the rates at which individuals move between compartments or leave infected compartments due to recovery or death. Elements V_{ij} of the matrix represent the transition rates between compartments. We ignore vaccination for adults γ for the calculation of R_0. Based on the compartment in Figure 1, we have

$$F = \begin{bmatrix} \beta SI \\ 0 \end{bmatrix}, \qquad V = \begin{bmatrix} \gamma E + \sigma E + \mu E \\ \delta I + \mu I - \sigma E \end{bmatrix}. \tag{5}$$

At the DFE matrices F and V are

$$F = \begin{bmatrix} 0 & \beta S \\ 0 & 0 \end{bmatrix}, \qquad V = \begin{bmatrix} \gamma + \sigma + \mu & O \\ -\sigma & \delta + \mu \end{bmatrix}. \tag{6}$$

The Next Generation Matrix G is constructed as

$$G = FV^{-1}, \tag{7}$$

where, V^{-1} represents the inverse of the matrix governing the transitions between infected states. with $V^{-1} = \begin{bmatrix} \frac{1}{\gamma+\sigma+\mu} & 0 \\ -\sigma & \delta+\mu \end{bmatrix}$, we have G as

$$G = \begin{bmatrix} \frac{\beta S\sigma}{\gamma+\sigma+\mu} & \frac{\beta S}{\delta+\mu} \\ 0 & 0 \end{bmatrix}. \tag{8}$$

The basic reproduction number R_0 is the spectral radius of the next generation matrix G. This is the largest absolute value of the eigenvalues of G. So G has eigenvalues 0 and R_0 where

$$R_0 = \frac{\beta S\sigma}{(\sigma+\mu)(\delta+\mu)}. \tag{9}$$

In the expanded SEIR model, where individuals in the E compartment are non-infectious, we assume that a fraction ρ of people are vaccinated upon entering the susceptible population through infant immunization programs. Adults also receive vaccinations at a rate of γ, ensuring they stay protected. With the total population held constant at 1, $(1-\rho)\mu N$ individuals join the susceptible group S, while ρN are directly moved to the recovered group R due to vaccination. The effective reproduction number under vaccination referred to as R_v, we obtain R_v as

$$R_v = \frac{\beta(1-\rho)\sigma}{(\gamma+\sigma+\mu)(\delta+\mu)}. \tag{10}$$

The result in (10) indicates that to reduce R_v below the critical threshold of one and achieve herd immunity, the proportion of the population that needs to be vaccinated must be greater than $1 - 1/R_0$ [10].

TABLE I: Parameter value.

Parameter	Value	Reference
μ	0.01241	[1]
σ	0.125	[13]
β	0.09091	[1]
γ	0%; 10%; 40%; 70%	Assumed
ρ	0%; 10%; 40%; 70%	Assumed
δ	0.14286	[13]

B. Sensitivity and elasticity

To establish effective control measures, we identify the key factors influencing disease transmission. By analyzing the sensitivity of the transmission rate, we determine which parameters have the strongest impact on the effective R_v. The sensitivity index of R_v with respect to a parameter ϕ is given by $\frac{\partial R_v}{\partial \phi}$. Another related measure is the elasticity index, which represents the normalized sensitivity index and describes the relative change in R_v with respect to ϕ. This elasticity index is denoted by

$$\Gamma_{\phi}^{R_v} = \frac{\partial R_v}{\partial \phi} \times \frac{\phi}{R_v}. \tag{11}$$

The significance of each parameter in terms of control can be assessed by calculating the elasticity indices. For equation 1-4 these are

$$\Gamma_{\gamma}^{R_v} = \frac{-\gamma}{\gamma+\sigma+\mu}, \tag{12}$$

$$\Gamma_{\rho}^{R_v} = \frac{-\rho}{1-\rho}. \tag{13}$$

The sign of the elasticity index shows if R_v rises (positive value) or falls (negative value) as the parameter ϕ changes, while the magnitude indicates how important that parameter is. These indices can help the design of control strategies by identifying the key parameters, though practical factors like cost and feasibility must also be considered [12].

III. Simulation results

To proceed with the simulation using the provided initial population values $S(0) = 100/165$, $E(0) = 40/165$, $I(0) = 15/165$, $R(0) = 10/165$ and parameters, we need to adjust the

TABLE II: Data on the impact of different vaccination strategies.

Adult Vaccination	Child Vaccination	Time to Reach Equilibrium	S	E	I	R	R_v	$\Gamma_{\gamma}^{R_v}$	$\Gamma_{\rho}^{R_v}$
0.0	0.0	248.79	0.9500	0.0000	0.0000	0.0500	0.54824	-0.0000	-0.0000
0.0	0.1	228.57	0.8500	0.0000	0.0000	0.1500	0.49342	-0.0000	-0.1111
0.0	0.4	119.04	0.5496	0.0001	0.0001	0.4503	0.32894	-0.0000	-0.6666
0.0	0.7	114.35	0.3492	0.0000	0.0000	0.6507	0.16447	-0.0000	-2.3333
0.1	0.0	43.79	0.0940	0.0001	0.0010	0.9049	0.31495	-0.4255	-0.0000
0.1	0.1	43.94	0.0850	0.0001	0.0009	0.9140	0.28345	-0.4255	-0.1111
0.1	0.4	44.37	0.0579	0.0001	0.0008	0.9412	0.18897	-0.4255	-0.6666
0.1	0.7	44.79	0.0308	0.0000	0.0007	0.9685	0.09448	-0.4255	-2.3333
0.4	0.0	26.27	0.0244	0.0000	0.0033	0.9723	0.13834	-0.7476	-0.0000
0.4	0.1	26.27	0.0219	0.0000	0.0033	0.9748	0.12450	-0.7476	-0.1111
0.4	0.4	26.25	0.0146	0.0000	0.0033	0.9821	0.08300	-0.7476	-0.6666
0.4	0.7	26.24	0.0073	0.0000	0.0033	0.9894	0.04150	-0.7476	-2.3333
0.7	0.0	24.55	0.0141	0.0000	0.0033	0.9826	0.08863	-0.8383	-0.0000
0.7	0.1	24.54	0.0127	0.0000	0.0033	0.9840	0.07977	-0.8383	-0.1111
0.7	0.4	24.54	0.0084	0.0000	0.0033	0.9883	0.05318	-0.8383	-0.6666
0.7	0.7	24.53	0.0042	0.0000	0.0033	0.9925	0.02659	-0.8383	-2.3333

initial conditions and incorporate the parameter values given in Table I.

The analysis of the impact of vaccination on the dynamics of measles, as illustrated in Figures 2-5 and supported by the data in Table II, provides crucial information on the interaction between the vaccination rates of adults and children. These figures represent different scenarios of vaccination coverage, allowing us to examine their influence on infection peaks, the time required to reach equilibrium, and the proportions of susceptible, exposed, infected and recovered populations. By comparing these outcomes, we can understand how targeted vaccination strategies alter the course of disease spread and contribute to epidemic control. In the following, each subfigure is analyzed in detail, highlighting its relationship with the corresponding numerical values in Table II.

The analysis of Figures 2a, 2b, 2c, and 2d offers significant insights into the impact of varying child vaccination rates on measles transmission dynamics in the absence of adult vaccination. In Figure 2a, where neither children nor adults are vaccinated (0% for both), the infection peak is observed at its highest level, and the system takes 248.79 units of time to stabilize, as presented in Table II. In this scenario, 95% of the population remains susceptible, while only 5% of the population transitions to the recovered state. This indicates that the majority of individuals remain vulnerable to the disease, allowing it to spread rapidly. The reproduction number is 0.548, which suggests a considerable potential for the disease to spread within the population. This highlights the importance of vaccination in mitigating disease transmission, as the absence of any form of vaccination results in a slow recovery and high infection rates.

When child vaccination is introduced at a rate of 10%, as shown in Figure 2b, a slight reduction in the infection peak is observed. This leads to a faster stabilization of the system, which now occurs in 228.57 units of time. In this case, 85% of the population remains susceptible, while 15% transitions to the recovered state. This results in a reduction in the susceptible population, which helps reduce the transmission dynamics. Additionally, the reproduction number decreases to 0.493, reflecting a moderate decrease in the spread of the disease. Although child vaccination at this level provides a positive impact, the reduction in infection rates is still not sufficient to achieve a rapid decline in transmission or prevent significant outbreaks.

In Figure 2c, with 40% child vaccination, the effect is much more pronounced. A substantial reduction in the infection peak is observed, and stabilization is achieved in 119.04 units of time. The proportion of the population that remains susceptible decreases significantly to 54.96%, while 45.03% of the population is now in the recovered state. This substantial shift indicates that a higher vaccination rate substantially reduces the pool of susceptible individuals, thereby curtailing the potential for large outbreaks. The reproduction number decreases further to 0.329, showing a marked reduction in the disease transmission potential. This demonstrates the importance of a higher child vaccination rate in significantly altering the trajectory of the disease and facilitating a faster recovery.

Finally, in Figure 2d, where 70% of children are vaccinated, the impact on the infection dynamics is striking. Infections are nearly suppressed, and stabilization occurs in just 114.35 units of time. Only 34.92% of the population remains susceptible, while 65.07% are in the recovered state. The reproduction number is reduced to 0.164, which reflects an almost complete control over the disease spread. The substantial reduction in both the susceptible population and the infection rate demonstrates the effectiveness of high vaccination coverage in controlling measles transmission and achieving herd immunity. This indicates that a 70% vaccination rate in children has a significant and profound effect on the progression of the disease, ensuring that most of the population is either immune

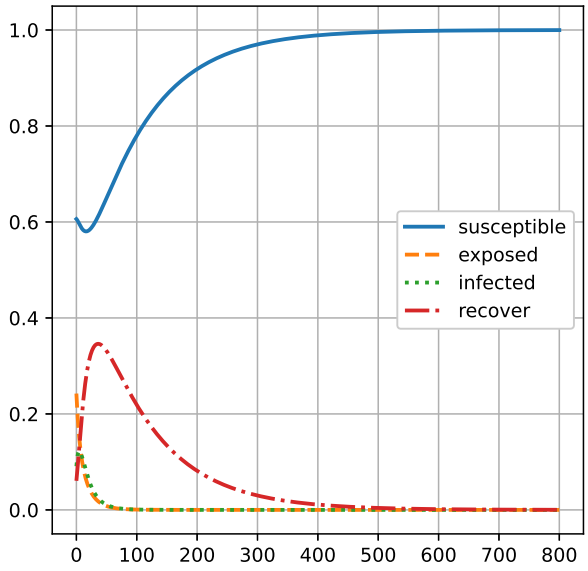

(a) No adult or child vaccination: highest infection peak with slow stabilization.

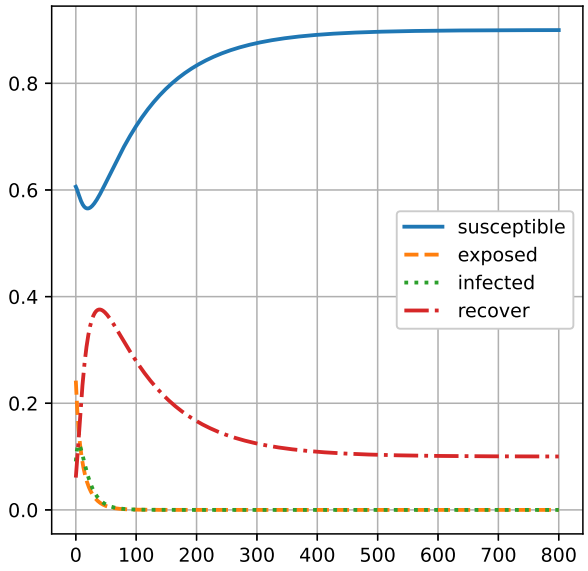

(b) 10% child vaccination: reduced infection peak and faster stabilization.

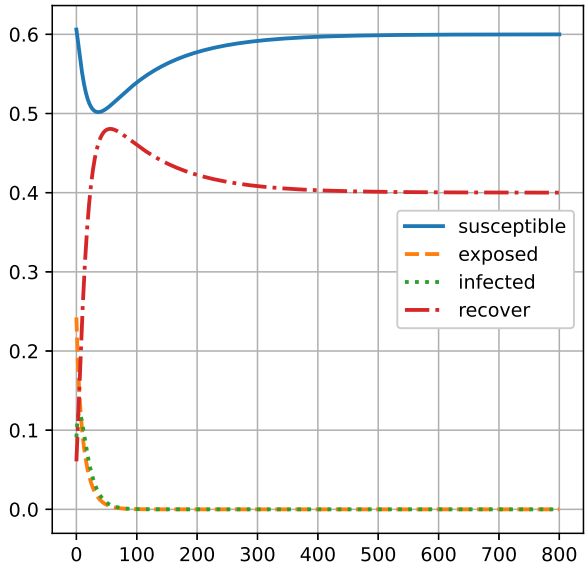

(c) 40% child vaccination: significant reduction in infections with improved stability.

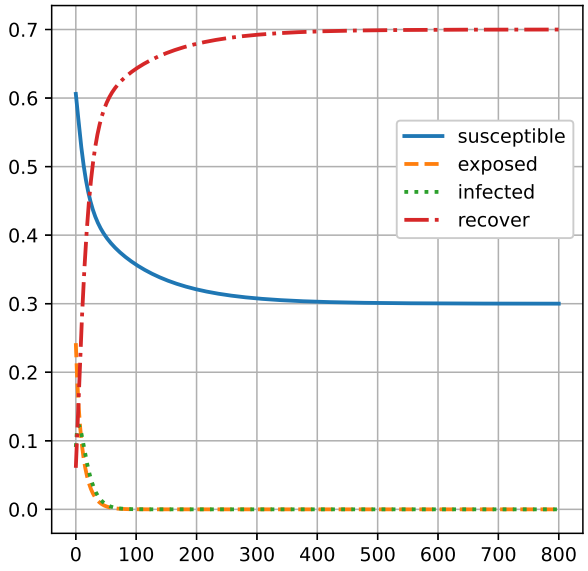

(d) 70% child vaccination: infections nearly eradicated, reaching equilibrium quickly.

Fig. 2: Measles dynamics with 0% adult and varying child vaccination.

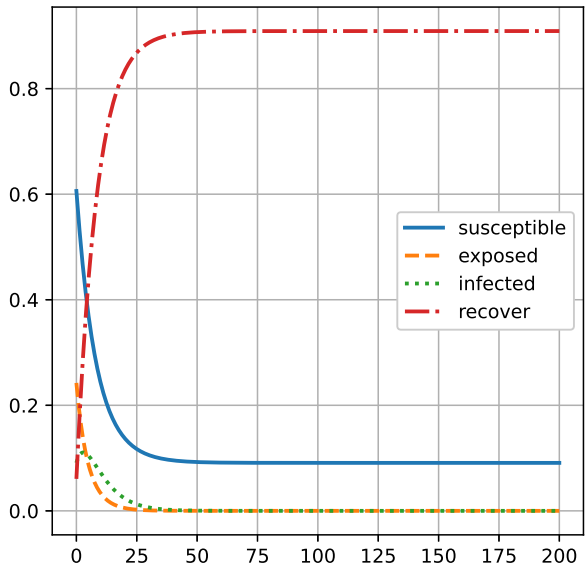

(a) 10% adult vaccination: moderate infection control with reduced peak.

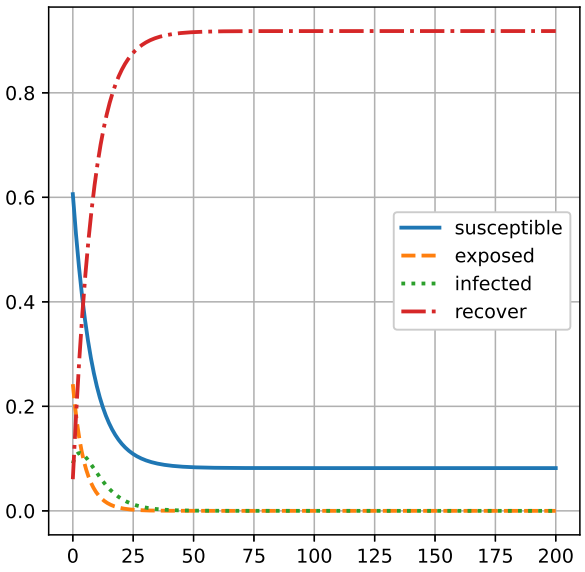

(b) 10% adult and 10% child vaccination: lower infection peak and faster stabilization.

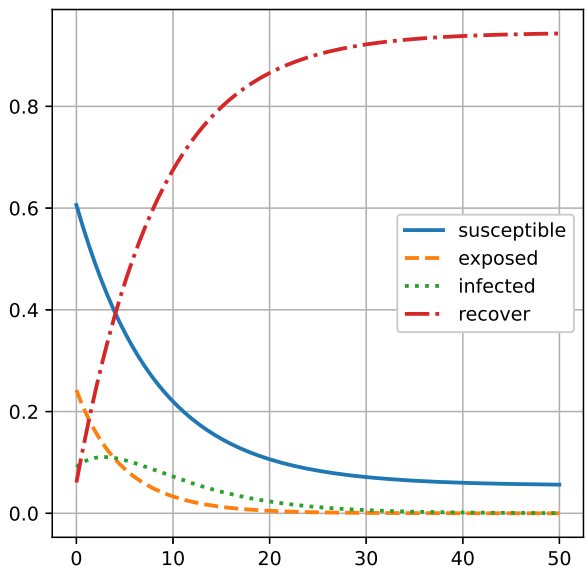

(c) 10% adult and 40% child vaccination: infections significantly suppressed.

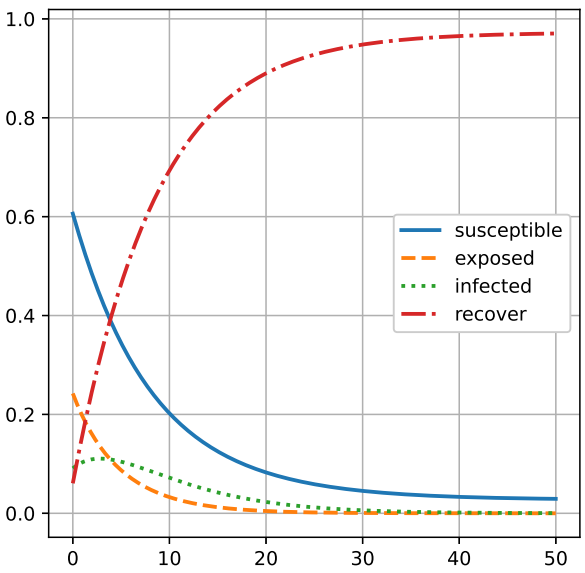

(d) 10% adult and 70% child vaccination: infections nearly eliminated.

Fig. 3: Measles dynamics with 10% adult and varying child vaccination.

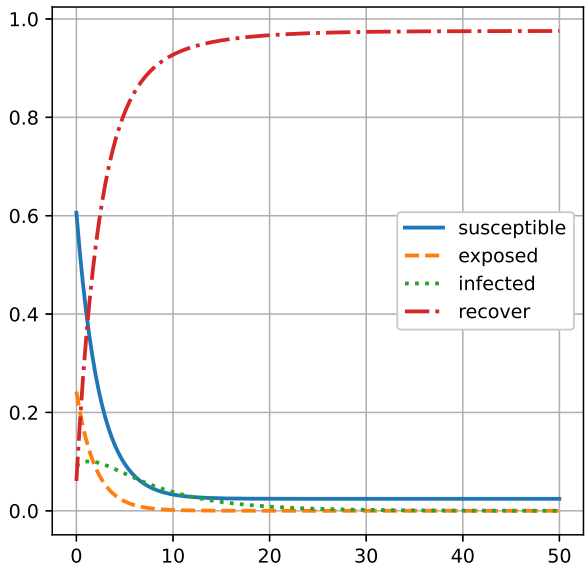

(a) 40% adult vaccination: infection peak reduced with quick stabilization.

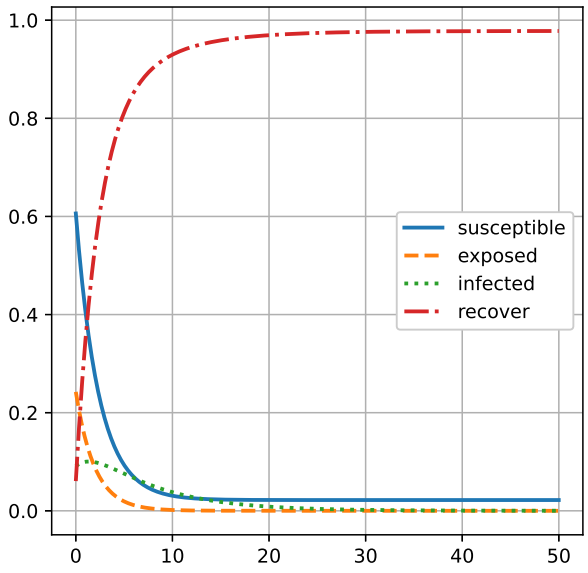

(b) 40% adult and 10% child vaccination: improved infection control.

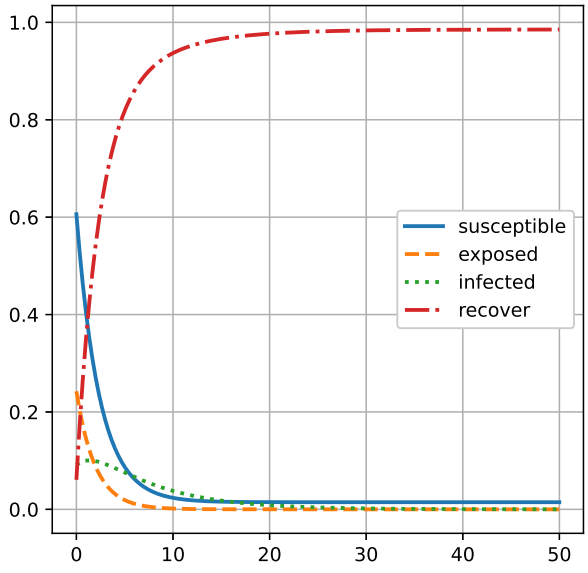

(c) 40% adult and 40% child vaccination: infections significantly minimized.

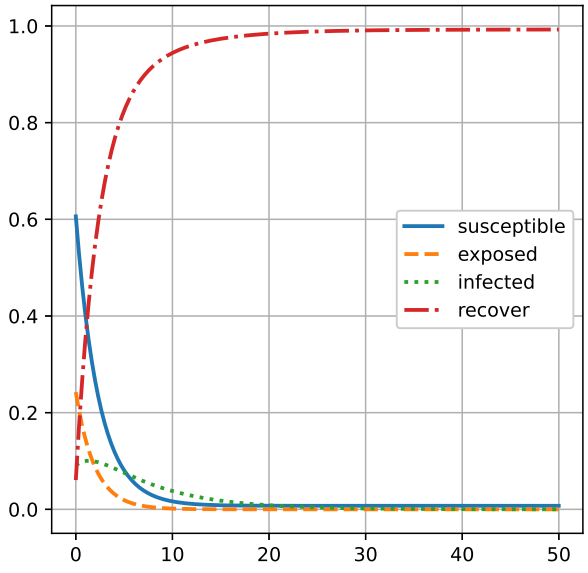

(d) 40% adult and 70% child vaccination: near-total suppression of infections.

Fig. 4: Measles dynamics with 40% adult and varying child vaccination.

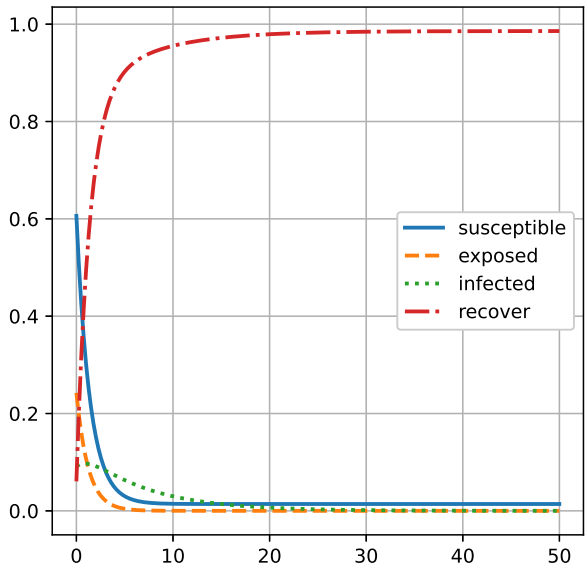

(a) 70% adult vaccination: infection nearly controlled with stable dynamics.

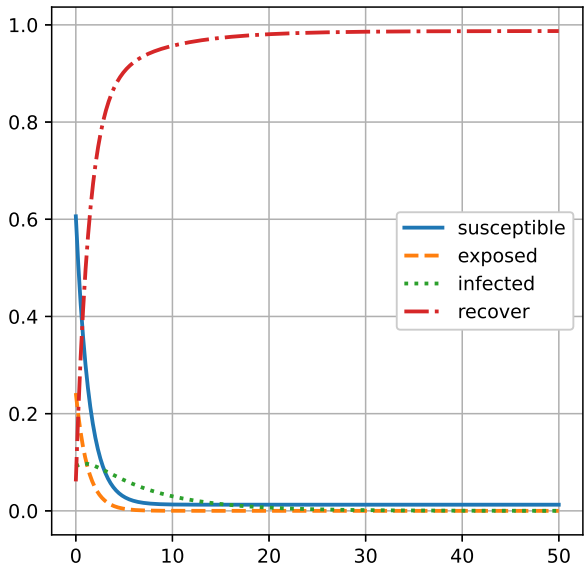

(b) 70% adult and 10% child vaccination: faster infection suppression.

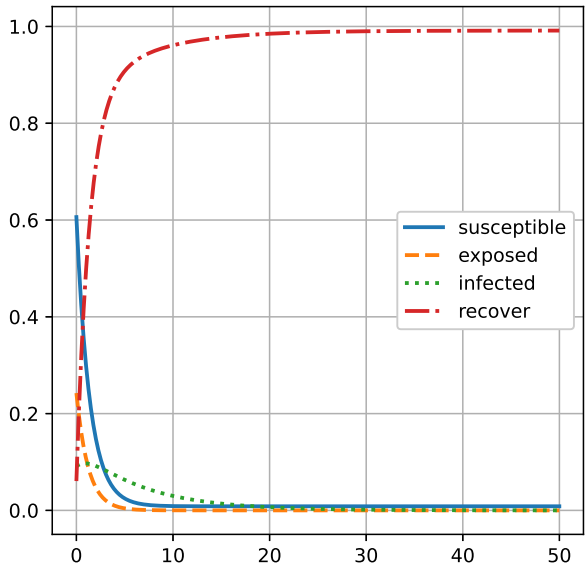

(c) 70% adult and 40% child vaccination: infections minimized with strong stability.

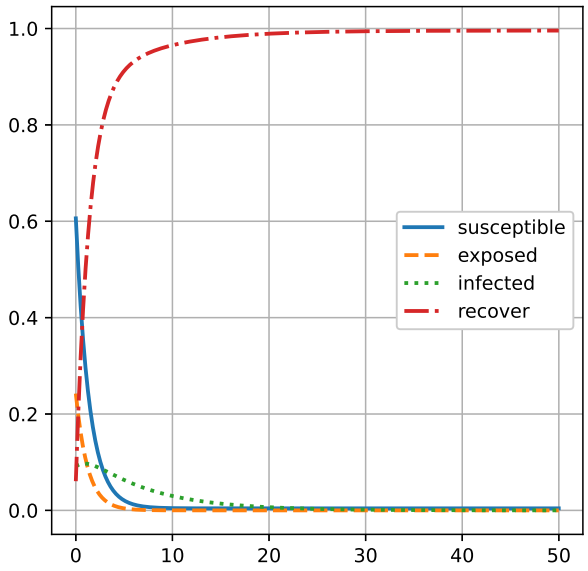

(d) 70% adult and 70% child vaccination: complete eradication of infections.

Fig. 5: Measles dynamics with 70% adult and varying child vaccination.

or recovered.

Figures 3a, 3b, 3c, and 3d further explore the impact of adding 10% adult vaccination in conjunction with varying child vaccination rates. In Figure 3a, where no child vaccination is implemented, a lower infection peak is observed compared to Figure 2a, with stabilization occurring in 43.79 units of time. The susceptible population is reduced to 9.4%, while 90.49% of the population has recovered. The reproduction number decreases to 0.314, indicating improved disease control due to the introduction of adult vaccination. This figure highlights the effectiveness of even a modest adult vaccination rate in reducing the infection burden.

When 10% child vaccination is added, as shown in Figure 3b, the stabilization time is slightly accelerated to 43.94 units, with the susceptible population decreasing to 8.5% and the recovered population increasing to 91.4%. The reproduction number decreases further to 0.283, demonstrating that the combined effect of adult and child vaccination results in a more effective control of the disease compared to adult vaccination alone. In Figure 3c, where 40% of children are vaccinated, stabilization occurs in 44.37 units, with 5.79% of the population susceptible and 94.12% recovered. The reproduction number decreases to 0.188, indicating a further reduction in transmission potential. This illustrates that combining moderate levels of adult and child vaccination accelerates disease control and facilitates a faster return to stability.

In Figure 3d, with 70% child vaccination and 10% adult vaccination, infections are nearly suppressed, with stabilization occurring in 44.79 units of time. Only 3.08% of the population remains susceptible, while 96.85% have recovered, and the reproduction number is reduced to 0.094. This combination results in near-total suppression of infections, indicating that combining both adult and child vaccination is highly effective in controlling the disease and minimizing its spread within the population.

Figures 4a, 4b, 4c, and 4d examine the impact of 40% adult vaccination combined with varying child vaccination rates. In Figure 4a, where no child vaccination is applied, the infection peak is significantly reduced compared to Figures 2a and 3a, and stabilization occurs in 26.27 units of time. Only 2.44% of the population remains susceptible, while 97.23% are in the recovered state. The reproduction number is 0.138, demonstrating that 40% adult vaccination provides a strong control over the disease. This figure shows that adult vaccination alone can dramatically reduce both the susceptible population and the infection rate, leading to rapid disease control.

The addition of 10% child vaccination, as shown in Figure 4b, maintains the stabilization time at 26.27 units. However, the proportion of susceptible individuals decreases further to 2.19%, while 97.48% of the population is recovered. The reproduction number decreases to 0.124, reflecting a continued improvement in disease control. In Figure 4c, where 40% child vaccination is added, stabilization occurs in 26.25 units of time, with 1.46% of the population susceptible and 98.21% recovered. The reproduction number decreases further to 0.083, indicating that both adult and child vaccinations work synergistically to reduce the disease transmission potential. In Figure 4d, where 70% of children are vaccinated, infections are nearly eliminated, and stabilization is achieved in 26.24 units of time. Only 0.73% of the population remains susceptible, while 98.94% have recovered, and the reproduction number is further reduced to 0.041. This demonstrates that higher adult vaccination rates, combined with significant child vaccination, result in highly effective disease control.

Figures 5a, 5b, 5c, and 5d explore the outcomes of 70% adult vaccination combined with varying child vaccination rates. In Figure 5a, where no child vaccination is implemented, infections are nearly eradicated, and stabilization occurs in 24.55 units of time. Only 1.41% of the population remains susceptible, while 98.26% of the population has recovered. The reproduction number is 0.088, suggesting that high adult vaccination alone is highly effective in controlling the disease. The system stabilizes quickly, and the susceptible population is minimal.

The introduction of 10% child vaccination, as seen in Figure 5b, slightly reduces the proportion of susceptible individuals to 1.27%, with 98.4% recovered, and the reproduction number decreases to 0.079. Stabilization still occurs in 24.54 units of time. In Figure 5c, with 40% child vaccination, stabilization occurs in 24.54 units of time, with only 0.84% of the population susceptible and 98.83% recovered. The reproduction number decreases to 0.053, further demonstrating the benefits of combining high adult vaccination rates with child vaccination. Finally, in Figure 5d, with 70% child vaccination, infections are entirely suppressed, with stabilization occurring in 24.53 units of time. Only 0.42% of the population remains susceptible, while 99.25% have recovered. The reproduction number is reduced to 0.026, confirming that the combination of 70% adult and 70% child vaccination leads to the most effective suppression of infections.

Finally, the results presented in Figures 2-5, alongside the data from Table II, emphasize the critical role of both adult and child vaccination in reducing infection rates, accelerating disease stabilization, and achieving herd immunity. While each group contributes individually to reducing the susceptible population and minimizing transmission, their combination is essential for achieving rapid and sustained control over the disease. The findings highlight the necessity of implementing vaccination programs targeting both children and adults to effectively mitigate the spread of infectious diseases, such as measles, and ensure long-term public health stability.

IV. Conclusion

In this paper, we demonstrate that both adult and child vaccination are essential in controlling the spread of measles, as analyzed through the SEIR mathematical model. Our results show that vaccinating children alone can significantly reduce infection rates and speed up stabilization. However, combining adult and child vaccination provides the most effective control, leading to faster stabilization, fewer infections, and

stronger immunity in the population. As vaccination coverage increases, the potential for disease transmission decreases. When both adult and child vaccination rates reach 70%, infections are nearly eradicated, highlighting the power of widespread vaccination in preventing outbreaks.

Our findings, based on the SEIR model, underscore the importance of implementing comprehensive vaccination programs that target both adults and children. Achieving high vaccination coverage is crucial to preventing future outbreaks and maintaining public health. In conclusion, this paper emphasizes the need for a combined vaccination strategy to reduce measles transmission and improve long-term public health outcomes, as demonstrated by the SEIR model's projections.

REFERENCES

[1] S. O. Sowole, A. Ibrahim, D. Sangare, and A. O. Lukman, "Mathematical model for measles disease with control on the susceptible and exposed compartments," *Open Journal of Mathematical Analysis*, vol. 4, no. 1, pp. 60–75, 2020.

[2] A. Abidemi, M. I. Abd Aziz, and R. Ahmad, "The impact of vaccination, individual protection, treatment and vector controls on dengue," *Engineering Letters*, vol. 27, no. 3, pp. 613–622, 2019.

[3] W. M. Getz and J. O. Lloyd-Smith, "Basic methods for modeling the invasion and spread of contagious diseases," *Disease evolution: models, concepts, and data analyses*, vol. 71, pp. 87–109, 2006.

[4] J. C. Butcher, *Numerical methods for ordinary differential equations*. John Wiley & Sons, 2016.

[5] H. T. Alemneh and A. M. Belay, "Modelling, analysis, and simulation of measles disease transmission dynamics," *Discrete Dynamics in Nature and Society*, vol. 2023, no. 1, pp. 1–20, 2023.

[6] M. El Hajji and A. H. Albargi, "A mathematical investigation of an "SVEIR" epidemic model for the measles transmission," *Math. Biosci. Eng*, vol. 19, pp. 2853–2875, 2022.

[7] E. A. Bakare, Y. Adekunle, and K. Kadiri, "Modelling and simulation of the dynamics of the transmission of measles," *International Jounal of Computer Trends and Technology*, vol. 3, pp. 174–178, 2012.

[8] S. O. Sowole, D. Sangare, A. A. Ibrahim, and I. A. Paul, "On the existence, uniqueness, stability of solution and numerical simulations of a mathematical model for measles disease," *Int. J. Adv. Math*, vol. 4, pp. 84–111, 2019.

[9] F. M. Guerra, S. Bolotin, G. Lim, J. Heffernan, S. L. Deeks, Y. Li, and N. S. Crowcroft, "The basic reproduction number (R_0) of measles: a systematic review," *The Lancet Infectious Diseases*, vol. 17, no. 12, pp. 420–428, 2017.

[10] P. Van den Driessche, "Reproduction numbers of infectious disease models," *Infectious disease modelling*, vol. 2, no. 3, pp. 288–303, 2017.

[11] R. Ramesh and G. A. Joseph, "The optimal control methods for the covid-19 pandemic model's precise and practical SIQR mathematical model." *IAENG International Journal of Applied Mathematics*, vol. 54, no. 8, pp. 1657–1672, 2024.

[12] C. A. Manore, K. S. Hickmann, S. Xu, H. J. Wearing, and J. M. Hyman, "Comparing dengue and chikungunya emergence and endemic transmission in A. aegypti and A. albopictus," *Journal of theoretical biology*, vol. 356, pp. 174–191, 2014.

[13] H. Trottier, H. Carabin, and P. Philippe, "Measles, pertussis, rubella and mumps completeness of reporting. literature review of estimates for industrialized countries," *Revue D'epidemiologie et de Sante Publique*, vol. 54, no. 1, pp. 27–39, 2006.